International Journal of Signal Processing, Image Processing and Pattern Recognition
Vol.7, No.1 (2014), pp.155-168
http://dx.doi.org/10.14257/ijsip.2014.7.1.15

Color Image Segmentation Algorithms based on Granular Computing Clustering

Hongbing Liu, Lei Li and Chang-an Wu

School of Computer and Information Technology, Xinyang Normal University, Xinyang 464000, P. R. China
liuhbing@126.com

Abstract

Color image segmentation algorithms are proposed based on granular computing clustering (GrCC). Firstly, the atomic hyperspherical granule is represented as the vector including the RGB value of pixel of color image and radii 0. Secondly, the union operator of two hyperspherical granules is designed to obtain the larger hyperspherical granule compared with these two hyperspherical granules. Thirdly, the granular computing clustering is developed by the union operator and the user-defined granularity threshold ρ. Global Consistency Error (GCE), Variation of Information (VI), Rand Index (RI), and Loss Entropy (ΔEn) are used to evaluate the segmentations. Segmentations of the color images selected from internet and BSD300 show that segmentations by GrCC speed up the segmentation process and achieve the better segmentation performance compared with Kmeans and FCM segmentations.

Keywords: *hyperspherical granule, granular computing, inclusion measure, fuzzy lattice, positive valuation function*

1. Introduction

In computer vision, image segmentation is the process of partitioning a digital image into multiple segments. The goal of segmentation is to simplify and/or change the representation of an image into something that is more meaningful and easier to analyze [1]. Image segmentation is typically used to locate objects and boundaries in images. More precisely, image segmentation is the process of assigning a label to every pixel in an image such that pixels with the same label share certain visual characteristics. The result of image segmentation is a set of segments that collectively cover the entire image, or a set of contours extracted from the image. Each of the pixels in a region is similar with respect to some characteristic or computed property, such as color, intensity, or texture. Adjacent regions are significantly different with respect to the same characteristic [1]. When applied to a stack of images, the resulting contours after image segmentation can be used to create 3D reconstructions with the help of interpolation algorithms. The practical applications of image segmentation included content-based image retrieval [2], machine vision [3], medical imaging [4], and object detection [5].

Clustering is a popular method by which an image is partitioned into multiple segments. Clustering can be considered the most important unsupervised learning problem, which deals with finding a structure in a collection of unlabeled data. Kmeans clustering and fuzz c-means (FCM) clustering are two important unsupervised algorithms. The K-means algorithm, which is computationally difficult (NP-hard), is an iterative technique that is used to partition an image into K clusters [6]. FCM is a data clustering technique where in each data point

ISSN: 2005-4254 IJSIP

belongs to a cluster to some degree that is specified by a membership grade. This technique was originally introduced by Jim Bezdek in 1981 [7] as an improvement on earlier clustering methods. It provides a method that shows how to group data points that populate some multidimensional space into a specific number of different clusters. FCM algorithm incorporates spatial information into the membership function for clustering. The spatial function is the summation of the membership function in the neighborhood of each pixel under consideration [8].

The present work uses granular computing clustering (GrCC) to form the color image segmentation algorithms. Granular computing (GrC) is an emerging computing paradigm of information processing. It concerns the processing of complex information entities called information granules, which arise in the process of data abstraction and derivation of knowledge from information.

The rest of this paper is presented as follows: Section 2 describes GrCC. Color image segmentation algorithms based on GrCC are described in Section 3. Section 4 demonstrates the segmentation results of color image selected from internet and BSD300. Section 5 summarizes the contribution of our work and presents future work plans.

2. Granular Computing Clustering Algorithm

Granular computing clustering (GrCC) algorithm is the method by which the granules are clusters. For the data set $S=\{x_i|i=1,2,...,n\}$ in N-dimensional space, we construct GrCC in terms of the following steps. Firstly, the single points in S is represented as the atomic granules which are indivisible. Secondly, the positive valuation function is introduced to form the inclusion measure function between two granules. Thirdly, the union operator is designed to update the granules.

2.1. GrCC

The idea of GrCC is described as follows. Firstly, the granule set (or the clustering set)(GS) is empty. Secondly, for the first datum x_1 in S, the corresponding atomic hyperspherical granule is represented as the hypersphere $G_1= (x_1,0)$ with the center x_1 and radii 0, and the center x_1 is regarded as the clustering center. The granule G_1 is move into GS, and the datum x_1 is removed from S. Thirdly, for the rest data $x_i(i=2,...,n)$, σ_{ij} represents the inclusion measure between the atomic hyperspherical granule G_i induced by the datum x_i and the hyperspherical granule G_j, if the σ_{ij} is maximal and the granularity of the union of G_i and G_j is less than or equal to the user-defined parameter ρ, the granule G_j in GS is replaced by the union of granule G_i and G_j, otherwise the atomic hyperspherical granule G_i becomes the member of GS, and x_i is removed from S until S is empty.

Algorithm1. GrCC

Input: the data set S, the user-defined parameter ρ of granularity

Output: the granule set (GS)

S1. initialize the granule set $GS=\varnothing$

S2. $i=1$

S3. for the ith sample x_i in S, form the corresponding atomic granule G_i

S4. $j=1$

S5. compute the inclusion measure σ_{ij} between the atomic granule G_i and the jth granule G_j in GS

S6. $j=j+1$

S7. find the maximal inclusion measure σ_{ik}

S8. if the granularity of the union of G_i and G_k is less than or equal to ρ, the granule G_k is replace by the union, otherwise G_i is the new member of *GS*.

S9. remove x_i until *S* is empty.

2.2. Inclusion Measure Function

In algorithm GrCC, the inclusion measure between a granule and the granules in *GS* and the granularity parameter ρ jointly control the union process of the atomic hyperspherical granule induced by the member of *S* and the hyperspherical granule in *GS*. A hyperspherical granule is represented as the sphere (x,r) with the center x and radii r in N-dimensional space, the atomic hyperspherical granule $(x,0)$ is induced by single point x. For two granules $G_1=(C_1,r_1)$ and $G_2=(C_2,r_2)$, the union operator and the intersection operator are designed as follows

$$G_1 \vee G_2=(P+Q, ||P-Q||)/2$$

where $P=C_1+ r_1/||C_{12}||$, $Q=C_2-r_2/||C_{12}||$, $C_{12}=C_2-C_1$.

$$G_1 \wedge G_2=(P+Q, ||P-Q||)/2$$

where $P=C_1+r_1/||C_{12}||$, $Q=C_2-r_2/||C_{12}||$, $C_{12}=C_2-C_1$. The union granule of two granules G_1 and G_2 is shown in Figure 1(a), and the intersection granule of two granules G_1 and G_2 is shown in Figure 1(b).

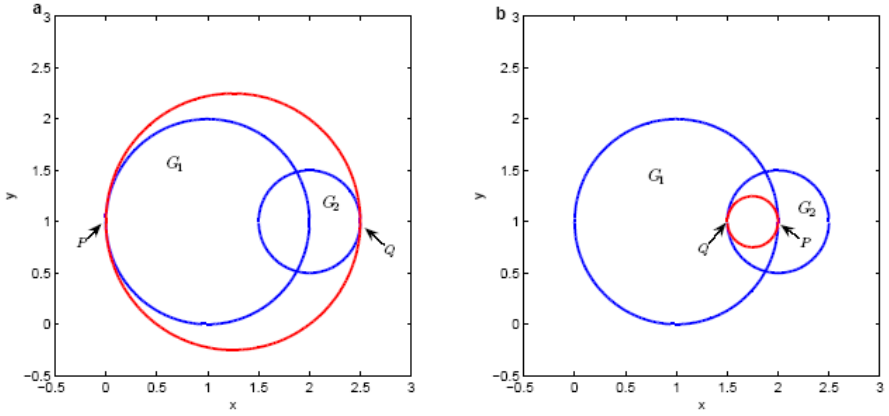

Figure 1. The Union Granule and Intersection Granule of Two Granules in 2-dimensional Space. (A) the Union Granule, (B) Intersection Granule

The inclusion relation between granules G_1 and G_2 and the operations between granules G_1 and G_2 satisfy

$$G_1 \subseteq G_2 \Leftrightarrow G_1=G_1 \wedge G_2,\ G_2=G_1 \vee G_2$$

The inclusion measure functions between G_1 and G_2 are induced by the union operator and intersection operator

$$\sigma(G_1,G_2)=v(G_1)/v(G_1 \vee G_2)$$

$$\mu(G_1,G_2)=v(G_1 \wedge G_2)/v(G_1)$$

$v(G)$ is called as the positive valuation function which is the mapping between granule space and real number space, and satisfies the two properties. (1) equality property: $G_1,G_2 \in GS$, $v(G_1)+v(G_2)=v(G_1 \vee G_2)+v(G_1 \wedge G_2)$, (2) inequality property: $G_1 \subset G_2 \Rightarrow v(G_1)<v(G_2)$.

The inclusion measure functions satisfies the following four properties

$$G \in GS,\ G \neq \varnothing \Rightarrow (G,\varnothing)=0$$

$$\forall G \Rightarrow (G,G)=1$$

$$G_1 \subseteq G_2 \Rightarrow (G,G_1) \leqslant (G,G_2)$$

$$G_1 \wedge G_2 \subset G_1 \Rightarrow (G_1,G_2)<1$$

According to the equality property and inequality property of $v(G)$ and aforementioned four properties of inclusion measure function, the increasing function can be taken as $v(G)$. So we define $v(G)$ as follows

$$v(G)=r$$

where $G=(x,r)$.

For granularity, the size of granule, such as the radii of granule, $2r$ is used to define the granularity.

The algebra system $\langle GS, \vee, \wedge, \sigma \rangle$ and $\langle GS, \vee, \wedge, \mu \rangle$ induced by GS, $\vee$, $\wedge$, σ and μ are fuzzy lattices.

3. Color Image Segmentation Algorithms Based on GrCC

RGB is an additive color model in which red, green, and blue light is added together in various ways to reproduce a broad array of colors. Given a color image represented by RGB, the color image segmentation based on GrCC includes the following steps.

Firstly, the data set is formed by the pixel values. Given a color image with 3×3 in Figure 2, the data set is formed by the vectors induced by the RGB value of pixel. The data set including 9 vector is

S={0.48 0.06 0.89, 0.75 0 0.75, 0 0.5 0, 0 0.75 0.75, 0.6 0.2 0, 0.17 0.51 0.34, 0.68 0.92 0.1, 0.85 0.7 1, 0.42 0.25 0.39}

Secondly, the algorithm GrCC is performed on the data set S, and the clustering granule set (GS) are achieved. The data set S is induced by the RGB, the granules are in the forms of spheres.

Thirdly, the color segmented image is reconstructed by the maximal inclusion measure. The reconstructed algorithm of the image I with $n_1 \times n_2$ on the clustering granule set GS is listed as follow.

Algorithm2. reconstructed algorithm

S1.for i=1:n_1

S2.for j=1:n_2

S3. the atomic granule G_{ij} is induced by the RGB value x of the pixel (i,j)

S4. for k=1:m

S5. computing the fuzzy inclusion measure $\sigma_{ij}(k)$ between G_{ij} and G_k

S6. end for k

S7. find the maximal fuzzy inclusion measure id=argmax($\sigma_{ij}(k)$) for k

S8. the color vector of the pixel (i,j) is replaced by the granule G_{id} in the clustering granule set

S9. end for j

S10. end for i

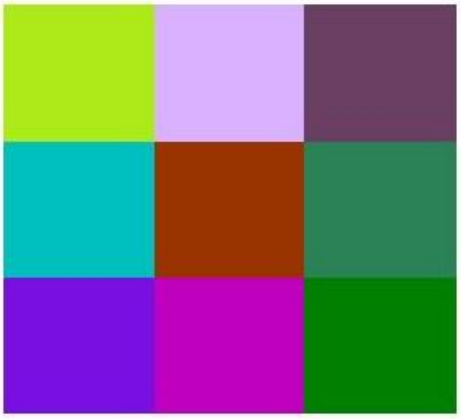

Figure 2. The 3×3 Image after 6000 Times Magnification

4. Evaluation of Segmentation

For the segmentations $S=\{S_1,S_2,...,S_n\}$ and $S'=\{S'_1,S'_2,...,S'_m\}$ of original color image I with n_1 rows and n_2 columns, and $N=|S_1|+|S_2|+...+|S_n|=|S'_1|+|S'_2|+...+|S'_m|$, we evaluate the segmentation by the following aspects.

4.1. Global Consistency Error

D. Martin proposed several error measures to quantify the consistency between image segmentations of differing granularity [9,10]. Let S and S' be two segmentations of an image $I=(x_1,x_2,...,x_N)$ consisting of N pixels. For a given pixel x_i, consider the classes (segments) that contain x_i in S and S'. We denote these sets of pixels by $C(S,x_i)$ and $C(S',x_i)$, respectively. Local Refinement Error (LRE) is then defined at point x_i as:

$$\mathrm{LRE}(S,S',x_i)=|C(S,x_i)-C(S',x_i)|/|C(S,x_i)|$$

where $C(S,x_i)-C(S',x_i)$ denotes the set differencing operator between sets $C(S,x_i)$ and $C(S',x_i)$. This error measure is not symmetric and encodes a measure of refinement in one direction only. There are two natural ways to combine the LRE at each point into a measure for the

entire image. Global Consistency Error (GCE) forces all local refinements to be in the same direction and is defined as:

$$GCE(S,S')=\min\{LRE(S,S',x_1)+\ldots+LRE(S,S',x_N), LRE(S',S,x_1)+\ldots+ LRE(S,S',x_N)\}/N$$

4.2. Variation of Information

Work in [11] computes a measure of information content in each of the segmentations. The proposed measure, termed the Variation of Information (VI), is a metric and is related to the conditional entropies between the class label distribution of the segmentations. The measure has several promising properties [11] but its potential for evaluating results on natural images where there is more than one ground-truth clustering is unclear. The VI is computed by the following steps. Firstly, computing the entropies En(S) and En(S') associated with segmentation S and S'.

$$E_n(S)=-(P(1)\log_2 P(1)+P(2)\log_2 P(2)+...+P(n)\log_2 P(n))$$

where $P(i)=|S_i|/N$

$$E_n(S')=-(P'(1)\log_2 P'(1)+P'(2)\log_2 P'(2)+...+P'(m)\log_2 P'(m))$$

Where $P'(i)=|S'_i|/N$, $\log_2 0=0$.

Secondly, computing the mutual information between S and S'

$$I(S,S')=\sum_{i=1}^{n}\sum_{j=1}^{m}P(i,j)\log_2\frac{P(i,j)}{P(i)P'(j)}$$

Thirdly, computing the VI

$$VI(S,S')=E_n(S)+E_n(S')-2I(S,S')$$

4.3. Rand Index

Rand Index (RI) was motivated by standard classification problems in which the result of a classification scheme has to be compared to a correct classification [12]. The most common performance measure for this problem calculates the fraction of correctly classified (respectively misclassified) elements to all elements. For Rand, comparing two clusters was just a natural extension of this problem which has a corresponding extension of the performance measure: instead of counting single elements he counts correctly classified pairs of elements. Thus, RI is defined by:

$$RI(S,S')=2(N_{11}+N_{00})/(N(N-1))$$

where N_{11} denotes the numbers of pairs that are in the same cluster under S and S', N_{00} denotes the number of pairs that are in different clusters under S and S'. RI depends on both the number of clusters and the number of elements, and ranges from 0 to 1. S and S' are identical when RI equals to 1.

4.4. Loss of Entropy

GCE, VI, and RI are used to measure the comparison of segmentation by algorithm and segmentation by human. If the human segmentation is known, we can compute the GEC, VI, and RI. If the human segmentation is unknown, we measure the segmentation by loss of entropy. For the segmentation by GrCC, the entropy of original image is computed by the following formula

$$En(S)=-(P_1\log_2 P_1+P_2\log_2 P_2+...+P_t\log_2 P_t)$$

t is the number of different RGB included in the image, $P_i=|S_i|/(n_1\times n_2)$, where S_i is the set including the pixels who have the same RGB value. The loss of entropy of segmentation (ΔEn) is the error of entropy between the original image and the segmentation is

$$\Delta\text{En}=\text{En}(I)-\text{En}(S)$$

5. Experiments

In order to verify the superiority of segmentation by spherical granular computing, we compared the proposed segmentation with segmentation by Kmeans and FCM, and all the experiments are performed in the same environment, such as Intel PIV PC with 2.8 GHz CPU and 2 GB memory, Microsoft Windows XP Professional and Matlab 7.0. The performance includes global consistency error (GCE), variant information (VI), rand index (RI), and loss of entropy (ΔEn).

Firstly, the complexity of segmentation is evaluated by the cpu time. Average faces (http://www.facedetection.com/facedetection/datasets.htm) are selected to perform the segmentation process. The female face image is selected to perform the algorithm 1 and the clustering granule set GS is obtained, and the male face image is selected to perform the algorithm 2. The segmentation complexity is evaluated by the cpu time, which is listed in Table 1. #cls is represented the number of clusters obtained by GrCC with the granularity threshold ρ, and used to perform the Kmeans and FCM. In general, #cls is greater than or equal to 2 for image segmentation. From the table, we can see cpu time consuming by Kmeans and FCM is more than cpu time consuming by GrCC. The average time consuming of GrCC, Kmeans, and GrCC is 0.1502 second, 0.9844 second, and 5.1647 second. Segmentation by GrCC accelerated 6.5520 (0.9844/0.1502) times compared with segmentation by Kmeans, and accelerated 34.3760 (5.1647/0.1502) times compared with segmentation by FCM. Standard deviations of segmentation cpu time by GrCC, Kmean, and FCM, are 0.0275, 0.8090, 6.2302. The stability of segmentation by GrCC is better than segmentation by Kmeans and FCM. Complexity of segmentation by GrCC is O(N) because granular computing clustering partitions the image by a single pass.

Secondly, images in BSD300 (http://www.eecs.berkeley.edu/Research/Projects/CS/vision /bsds/), which includes original color images and their human segmentations, is selected to perform segmentations by GrCC, Kmeans, and FCM, the segmentation performance is evaluated by GCE, VI, and RI.

For the color image 3096 in BSD300, Figure 3 includes the original image and the boundary of human segmentation. The parameter of granularity are set from 0.6 to 0.3 with the step 0.02, the number of corresponding hyperspherical granule is selected as the number of cluster for Kmeans and FCM. GCE, VI, and RI by GrCC, Kmeans, and FCM are listed in table 2. GrCC achieved the best segmentation, the minimal GCE (0.0211) by GrCC is less than the minimal GCE (0.0236) by Kmeans and the minimal GCE(0.0252) by FCM, the minimal VI (0.1520) by GrCC is less than the minimal VI (0.1711) by Kmeans and the minimal VI (0.1801) by FCM, the maximal RI by GrCC is 0.9746, which is great than maximal RI (0.9730) by Kmeans and the maximal RI (0.9719) by FCM. On the other hand, for the same parameter, such as ρ and #cls induced by GrCC, the GCE, VI, and RI by GrCC are better than Kmean and FCM. Therefore, the segmentation by GrCC is better than segmentation by Kmeans and FCM from GCE, VI, and RI. The boundaries of the best segmentations of by GrCC, Kmeans, and FCM are shown in figures Figure 4, Figure 5, and Figure 6, from the figures, we can see the segmentations by GrCC is superior to the segmentations by Kmeans and FCM from the sense of sight.

We also selected the other color images from the BSD300, such as image 135069, image 302003, and image 35070, to perform GrCC. The segmentations and boundaries are shown in Figure 7, Figure 8, and Figure 9. The segmentations are satisfactory from the sense of sight.

Thirdly, the color images selected from internet are performed by GrCC. Because the human segmentation does not exist, the segmentation is evaluated by loss of entropy for the color images selected from internet at random. The loss of entropy increases with the increasing of the granularity parameter ρ of GrCC. Figure 10, Figure 11, and Figure 12 show the original images and segmentations by GrCC.

6. Conclusions

A new segmentation of color image is proposed based on granular computing clustering algorithm. The segmentation experimental results shown that (1) GrCC segmentation is a quick segmentation compared with Kmeans and FCM segmentations, (2) GrCC segmentation is better than Kmeans and FCM from the aspects of GCE, VI, and RI. (3) loss of entropy only is a numerical measure for the segmentation of color image without the corresponding human segmentation. Some issues still need further study, such as the adaptive selection of granularity threshold ρ, the further analysis of loss entropy.

Table 1. The cpu Time of Segmentations for Average Faces

ρ	#cls	GrCC	Kmeans	FCM
0.95	2	0.1094	0.2969	1.6406
0.90	2	0.1250	0.4531	1.9375
0.85	2	0.1563	0.2656	1.7031
0.80	3	0.1250	0.7031	3.0938
0.75	3	0.1406	0.7344	2.9688
0.70	3	0.1563	0.8438	2.7813
0.65	3	0.2188	0.8594	2.6875
0.60	3	0.1406	0.5781	2.8750
0.55	3	0.1563	0.9063	2.7188
0.50	4	0.1406	0.9531	7.4375
0.45	3	0.1406	1.0313	2.6250
0.40	5	0.1719	1.8438	10.5938
0.35	7	0.1719	3.3281	24.0781

Table 2. The Performance of Segmentations for Image 3096 in BSD300

ρ	#cls	GrCC			Kmeans			FCM		
		GCE	VI	RI	GCE	VI	RI	GCE	VI	RI
0.60	2	0.0211	0.1520	0.9746	0.0236	0.1711	0.9730	0.0252	0.1801	0.9719
0.58	2	0.0211	0.1520	0.9746	0.0236	0.1711	0.9730	0.0252	0.1801	0.9719
0.56	2	0.0211	0.1520	0.9746	0.0236	0.1711	0.9730	0.0252	0.1801	0.9719
0.54	2	0.0211	0.1520	0.9746	0.0236	0.1711	0.9730	0.0252	0.1801	0.9719
0.52	2	0.0211	0.1520	0.9746	0.0236	0.1711	0.9730	0.0252	0.1801	0.9719
0.50	2	0.0211	0.1520	0.9746	0.0236	0.1711	0.9730	0.0252	0.1801	0.9719
0.48	2	0.0211	0.1520	0.9746	0.0236	0.1711	0.9730	0.0252	0.1801	0.9719
0.46	3	0.0211	0.1520	0.9746	0.0264	0.9925	0.6128	0.0264	1.0256	0.5920
0.44	3	0.0211	0.1520	0.9746	0.0264	0.9925	0.6128	0.0264	1.0256	0.5920
0.42	3	0.0211	0.1520	0.9746	0.0264	0.9925	0.6128	0.0264	1.0256	0.5920
0.40	3	0.0308	0.1520	0.9746	0.0264	0.9925	0.6128	0.0264	1.0256	0.5920
0.38	3	0.0308	0.3956	0.9168	0.0264	0.9925	0.6128	0.0264	1.0256	0.5920
0.36	3	0.0308	0.5029	0.8924	0.0264	0.9925	0.6128	0.0264	1.0256	0.5920
0.34	3	0.0308	0.5029	0.8924	0.0264	0.9925	0.6128	0.0264	1.0256	0.5920
0.32	4	0.0308	0.5029	0.8924	0.0273	1.5245	0.4539	0.0275	1.5400	0.4484
0.30	4	0.0308	0.5029	0.8924	0.0273	1.5307	0.4517	0.0275	1.5400	0.4484

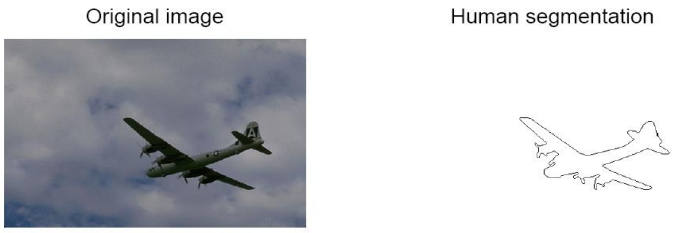

Figure 3. The Original Image and Human Segmentation of Image 3096 in BSD300

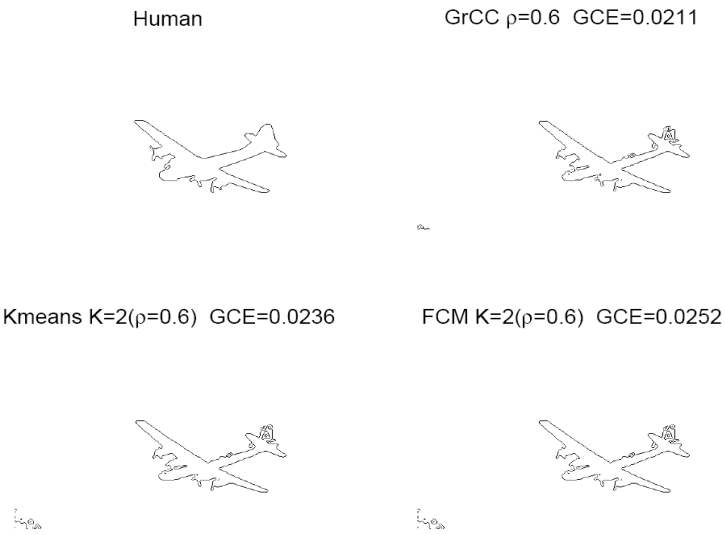

Figure 4. Boundaries of Segmentations by Human, GrCC, Kmeans, and FCM with Minimal GCE

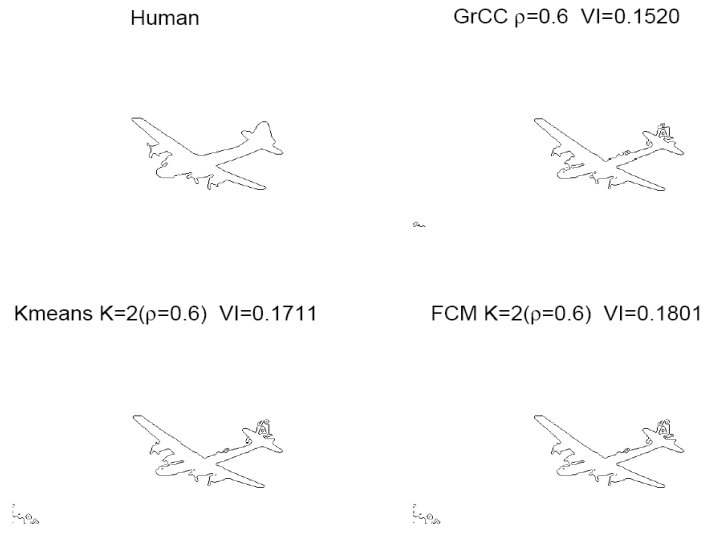

Figure 5. Boundaries of Segmentations by Human, GrCC, Kmeans, and FCM with Minimal VI

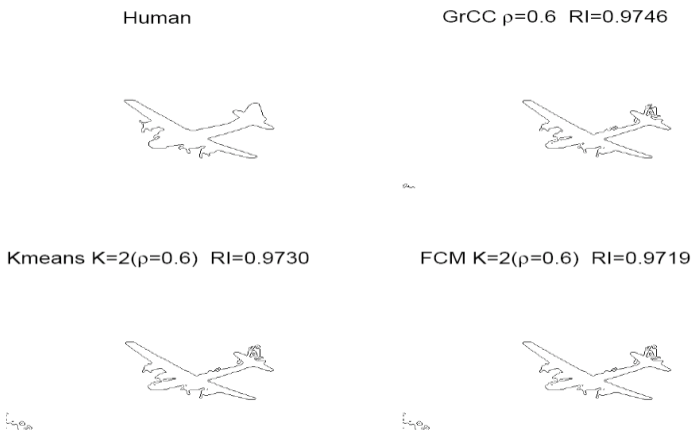

Figure 6. Boundaries of Segmentations by Human, GrCC, Kmeans, and FCM with Maximal RI

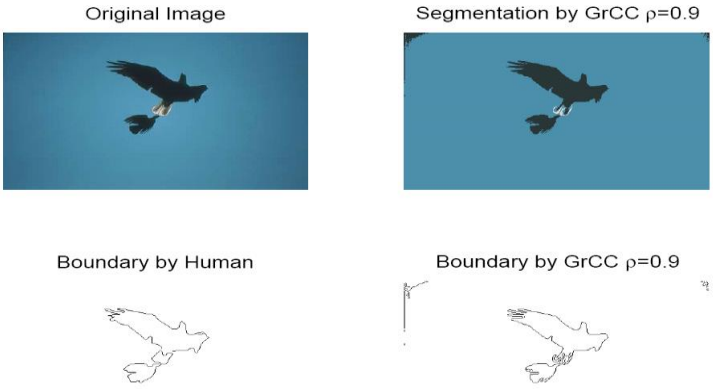

Figure 7. Segmentations by GrCC for Image 135069 in BSD300

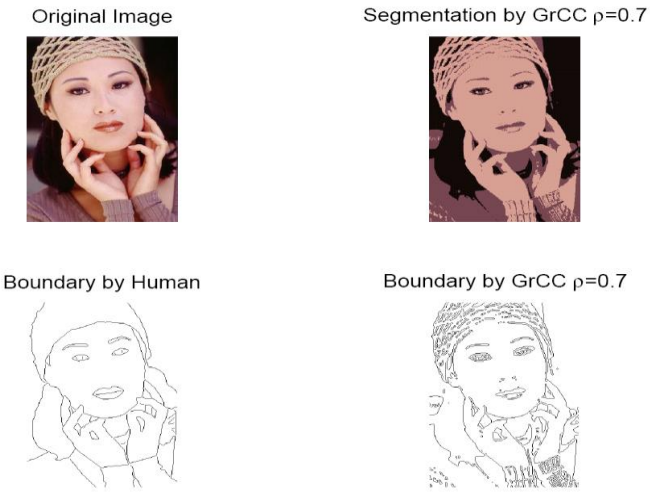

Figure 8. Segmentations by GrCC for image 302003 in BSD300

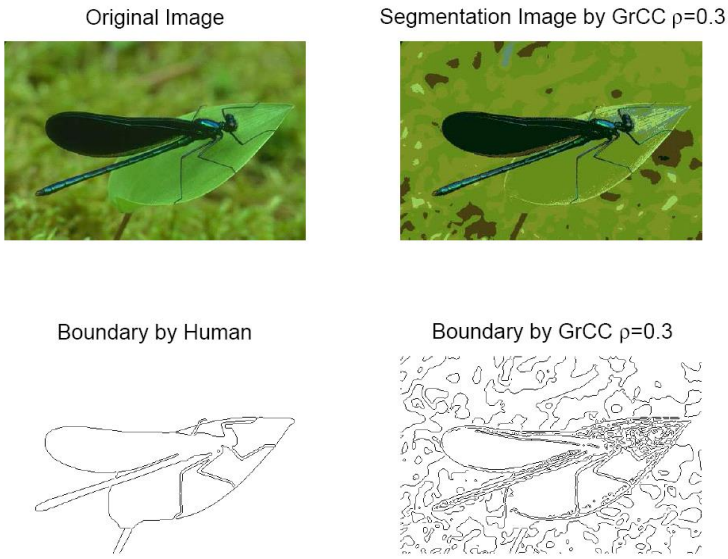

Figure 9. Segmentations by GrCC for Image 35070 in BSD300

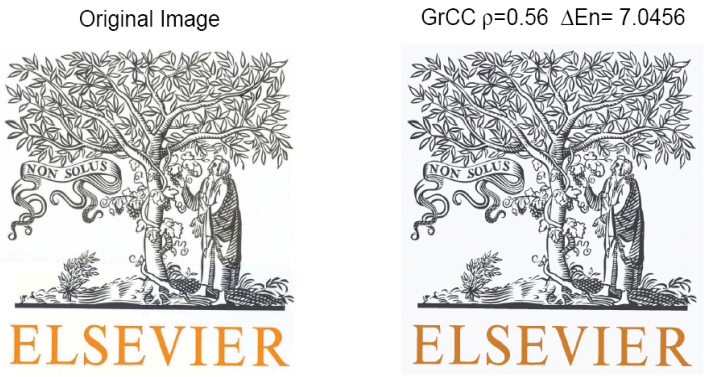

Figure 10. Segmentations by GrCC for Image Selected from Internet

Figure 11. Segmentations by GrCC for Image Selected from Internet

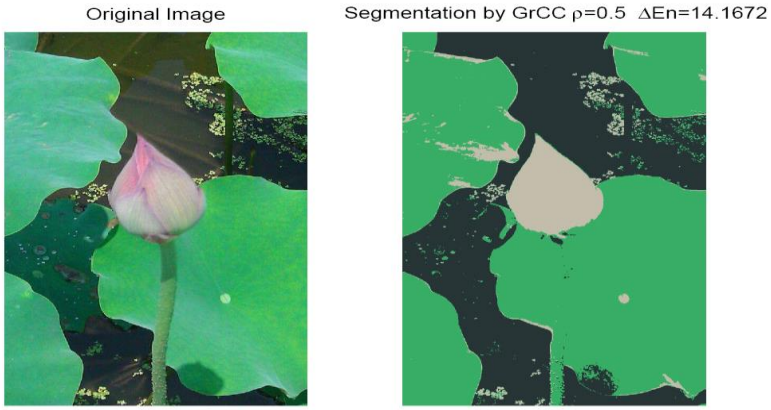

Figure 12. Segmentations by GrCC for Image Selected from Internet

Acknowledgment

This work was supported in part by the Natural Science Foundation of China (Grant No. 61170202) and Natural Science Foundation of Henan (No. 132300410421).

References

[1] L. G. Shapiro, G. C. Stockman. Computer Vision. New Jersey, Prentice-Hall (2001).
[2] M. S. Lew, N. Sebe, C. Djeraba, R. Jain. Content based multimedia information retrieval: State of the art and challenges, ACM Transactions on Multimedia Computing, Communications and Applications, 2(1): 1-19 (2006).
[3] F. D. Turek. Machine vision fundamentals, How to make robots see, NASA Tech Briefs 35 (6): 60-62 (2011).
[4] D. L. Pham, C. Xu, J. L. Prince. Current methods in medical image segmentation, Annual Review of Biomedical Engineering, 2: 315-337(2000).
[5] F. Fleuret, J. Berclaz, R. Lengagne, and P. Fua. Multi-camera people tracking with a probabilistic occupancy map, IEEE Transactions on Pattern Analysis and Machine Intelligence, 30(2):267-282 (2008)
[6] D. Aloise, A. Deshpande, P. Hansen, P. Popat. NP-hardness of Euclidean sum-of-squares clustering, Machine Learning, 75: 245-249 (2009).
[7] R. P. Nikhil, J. C. Bezdek. On cluster validity for the fuzzy c-means model, IEEE Transactions on Fuzzy Systems, 3(3):370-379 (1995).
[8] K.-S. Chuang, H.-L. Tzeng, S. Chen, J. Wu, T. J. Chen. Fuzzy c-means clustering with spatial information for image segmentation, Computerized Medical Imaging and Graphics, 30(1):9-15 (2006).
[9] D. Martin. An empirical approach to grouping and segmentation, Ph.D. dissertation, University of California, Berkeley, 2002.
[10] D. R. Martin, C. Fowlkes, J. Malik. Learning to detect natural image boundaries using local brightness, color, and texture cues, IEEE Transaction Pattern Analysis Machine Intelligence, 26(5): 530-549 (2004).
[11] M. Meilă. Comparing clusterings an information based distance. Journal of Multivariate Analysis, 98(5):873-895 (2007).
[12] W. M. Randm. Objective criteria for the evaluation of clustering methods. Journal of the American Statistical Association, 66(336):846-850 (1971).

Author

Hongbing Liu, received his Ph.D. degree from Wuhan University of Technology in 2011. He is an associate professor at Xinyang Normal University. His research interests include intelligent information processing, data mining, rough set and image processing, etc.